ISBN: 978-3-95450-227-1 ISSN: 2673-5490 doi:10.18429/JACoW-IPAC2022-WEPOPT013

EFFECT OF A SPURIOUS CLIQ FIRING ON THE CIRCULATING BEAM IN HL-LHC*

C. Hernalsteens, M. V. Basco, O. K. Tuormaa,
B. Lindstrom, E. Ravaioli, C. Wiesner, D. Wollmann
CERN, Geneva, Switzerland

Abstract

The High Luminosity LHC (HL-LHC) will reach a nominal, levelled luminosity of 5×10^{34} cm^{-1} s^{-2} and a stored energy of nearly 700 MJ in each of the two proton beams. The new large-aperture final focusing Nb_3Sn quadrupole magnets in IR1 and IR5, which are essential to achieve the luminosity target, will be protected using the novel Coupling Loss Induced Quench (CLIQ) system. A spurious discharge of a CLIQ unit will impact the circulating beam through higher order multipolar field components that develop rapidly over a few turns. This paper reports on dedicated beam tracking studies performed to evaluate the criticality of this failure on the HL-LHC beam. Simulations for different machine and optics configurations show that the beam losses reach a critical level after only five machine turns following the spurious CLIQ trigger, which is much faster than assumed in previous simulations that did not consider the higher order multipolar fields. Machine protection requirements using a dedicated interlock to mitigate this failure are discussed.

INTRODUCTION

The High Luminosity upgrade will increase the levelled luminosity of the CERN Large Hadron Collider (LHC) to 5×10^{34} cm^{-2} s^{-1} [1] by means of a higher beam brightness and using new equipment to reduce the β-function at the interaction points (IPs) (the so-called β^*) for the ATLAS and CMS experiments. The intensity increase means that the total stored beam energy will increase to 674 MJ for the nominal parameters for each of the two circulating beams [1]. This has a critical impact on machine protection systems of the LHC, which must ensure that the beams are extracted safely before uncontrolled beam losses would lead to equipment damage. In addition, the multi-stage collimation system of HL-LHC will feature a Hollow-Electron Lens (HEL) to reduce the beam halo population [2] by increasing the diffusion speed within the beam halo [3]. The halo population has a direct impact on the dynamics of the induced beam losses which in turn impacts the criticality of fast failures and requires detailed beam tracking studies to evaluate the evolution of beam losses [4].

The new equipment allowing to reduce the β^* down to 15 cm includes the large aperture superconducting final focusing quadrupole magnets (triplets). The active magnet protection of these magnets features the novel Coupling Loss Induced Quench (CLIQ) system [5]. The CLIQ magnet protection system will be used in the electrical circuit of the final focusing triplet quadrupoles around ATLAS (IP1) and CMS (IP5). Upon quench detection, the CLIQ discharge is activated, causing an additional and unbalanced current in the magnet poles, as compared to the nominal current. In the case of a spurious discharge of a CLIQ unit with circulating beams, the beam will be perturbed by the resulting multipolar magnetic field [6] at locations featuring very large β-functions and large amplitude of the crossing angle bump which increases the sensitivity to the field perturbation, as shown in Fig. 1. Initial studies of this failure case led to the modification of the CLIQ connection scheme so that the main field component became skew octupolar [7]. We report on beam tracking studies using the FailSim framework [8] which show that a spurious CLIQ discharge is the most critical fast failure identified for HL-LHC. The beam losses as a function of time are compared for different machine configurations to derive requirements on the interlock mechanism that needs to be developed to protect against such failure.

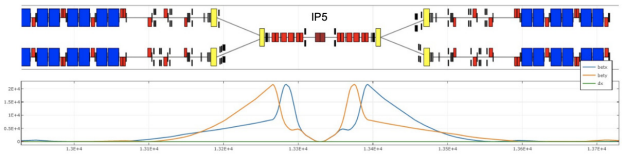

Figure 1: Horizontal (blue) and vertical (orange) β-functions around IP5. The β^* reaches 15 cm at the IP and over 20 km in the triplet region (shown as red boxes on both sides of the IP). Blue boxes represent main dipole magnets while yellow boxes represent the separation and recombination dipoles.

MACHINE, BEAM AND OPTICS MODELS

The nominal simulation setup uses the HL-LHC lattice V1.4 with the most critical optics configuration for round beams with $\beta^* = 15$ cm. We consider a full machine with 2736 bunches at top energy, as shown in Table 1. The baseline collimation scenario with the primary collimators (TCPs) cut set at 6.7 σ is compared with a collimation scheme with a TCP cut set at 8.5 σ[1]. The multipolar decomposition of the field components induced by the CLIQ discharge are reported in detail in [6]. The model of the transverse beam distribution is based on Run II beam scraping measurements performed to characterize the distribution and its halo up to the TCPs [9]. A fit on the measurement characterizes the transverse distribution as the sum of two Gaussian distributions which we extended to form the radial distribution over the 4D normalized transverse phase space

* Research supported by the HL-LHC project.

[1] For the relaxed collimation settings we use the HL-LHC lattice V1.5.

ISBN: 978-3-95450-227-1 ISSN: 2673-5490 doi:10.18429/JACoW-IPAC2022-WEPOPT013

Table 1: Machine and beam parameters for the squeezed HL-LHC optics, as used in the simulations.

Parameter	HL-LHC
Energy	7 TeV
Stored beam energy	674 MJ
Bunch intensity (2736 bunches)	2.2×10^{11} p^+
Normalized emittance	2.5 µm
β^* at IP1-5	15 cm
Crossing angle at IP1-5	500 µrad
Primary collimator (TCP) cut	6.7 σ or 8.5 σ
HEL inner radius	4.7 σ or 6.5 σ

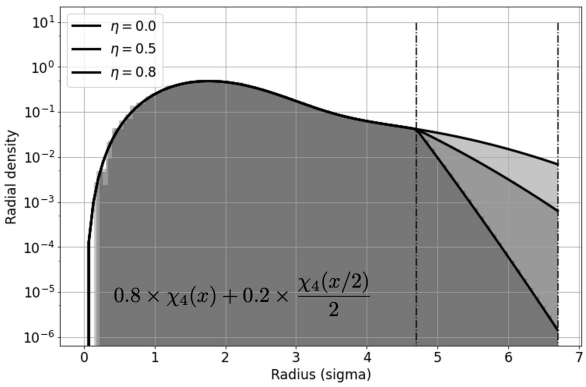

Figure 2: Radial distribution function in the 4D transverse phase space. The distribution follows the sum of two χ distributions. From the HEL inner radius up to the cut radius imposed by the primary collimators, an exponential decrease factor is added to account for the halo depletion. Three levels of depletion are shown, starting from $\eta = 0$ (no depletion) up to $\eta = 0.8$ corresponding to an 80% population decrease.

[4]. To account for the halo depletion induced by the HEL, this distribution function is modified by a decreasing exponential function within the HEL active radii - from the inner radius up to ρ_{TCP}, the radius at which the primary collimators are set - and then re-normalized. The halo depletion factor η represents the relative depletion in the halo. The resulting radial density is shown in Fig. 2. To perform the simulations, the distribution is sampled uniformly inside a 4D hypersphere with a radius equal to ρ_{TCP}. A weight is associated to each particle during the analysis, allowing the results to be recomputed for different values of η. The beam distribution is tracked using the time-dependent multipolar decomposition of the field induced by the CLIQ discharge. The beam losses and the surviving particles are recorded at each turn.

BEAM LOSSES FROM SPURIOUS CLIQ DISCHARGE

A simulation was performed for the spurious discharge of a single CLIQ unit for each triplet magnet in IR1 and IR5. The Q2 magnet furthest from the IP on the right side, i.e. Q2b, of IP5 is found to be the most critical case for Beam 1,

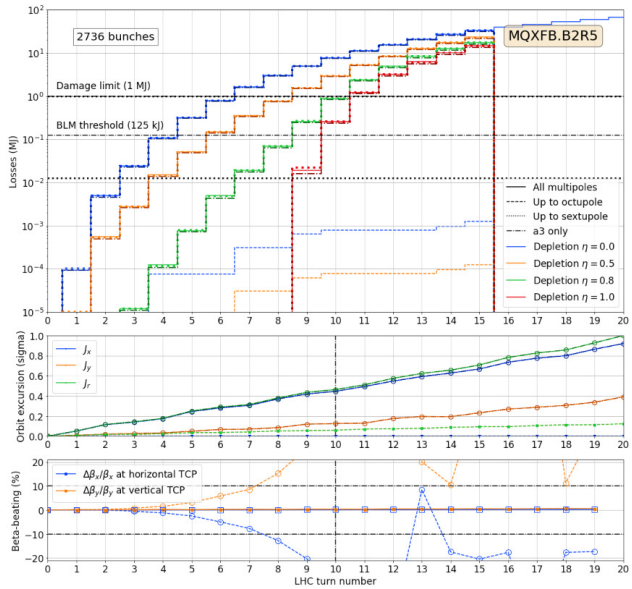

Figure 3: Beam losses (top), orbit excursion (center) and β-beating (bottom) as function of the turn number. The CLIQ discharge starts at turn one. For the beam losses, the color scheme depicts four different halo depletion parameters. The order of truncation of the multipoles is shown using different line styles. The damage limit (1 MJ) and the BLM threshold (125 kJ) are also shown. The orbit excursion, in both transverse planes, and as a 4D amplitude is shown following the same line styles convention as for the beam losses. The horizontal (resp. vertical) β-beating is shown at the location of the horizontal (resp. vertical) TCP.

leading to the fastest and largest beam losses. The time-dependent cumulative beam loss profiles are shown in Fig. 3. The critical loss level is also indicated, with the beam losses reaching that level within 10 turns or less depending on the beam halo depletion. The interlocking threshold of the beam loss monitors (BLM), set at 125 kJ is also visible [10]. As the losses are much faster and larger than initially expected [6], a systematic study was performed to understand their origin. The CLIQ multipoles were limited in simulation to different order (up to sextupole, up to octupole or up to dodecapole), with each result depicted in Fig. 3. The beam losses are shown to be minimal when limiting to the sextupolar component and critical for the other multipolar expansions. This indicates that the skew octupolar component, the larger multipole, dominates the dynamics and is responsible for the beam losses. This is confirmed when observing the orbit excursion (middle plot) and the β-beating (bottom plot). The orbit excursion itself cannot explain the large observed beam losses. An excursion of about 1.5 σ would be required to reach losses of 1 MJ. The β-beating is negligible and remains under 10% up to turn 7, where the losses already exceed the critical level. The loss mechanism is therefore not coming from an orbit excursion driving the beam to the TCPs nor from a beam envelope change reducing the normalized aperture. The beam distribution in physical space has

ISBN: 978-3-95450-227-1 ISSN: 2673-5490 doi:10.18429/JACoW-IPAC2022-WEPOPT013

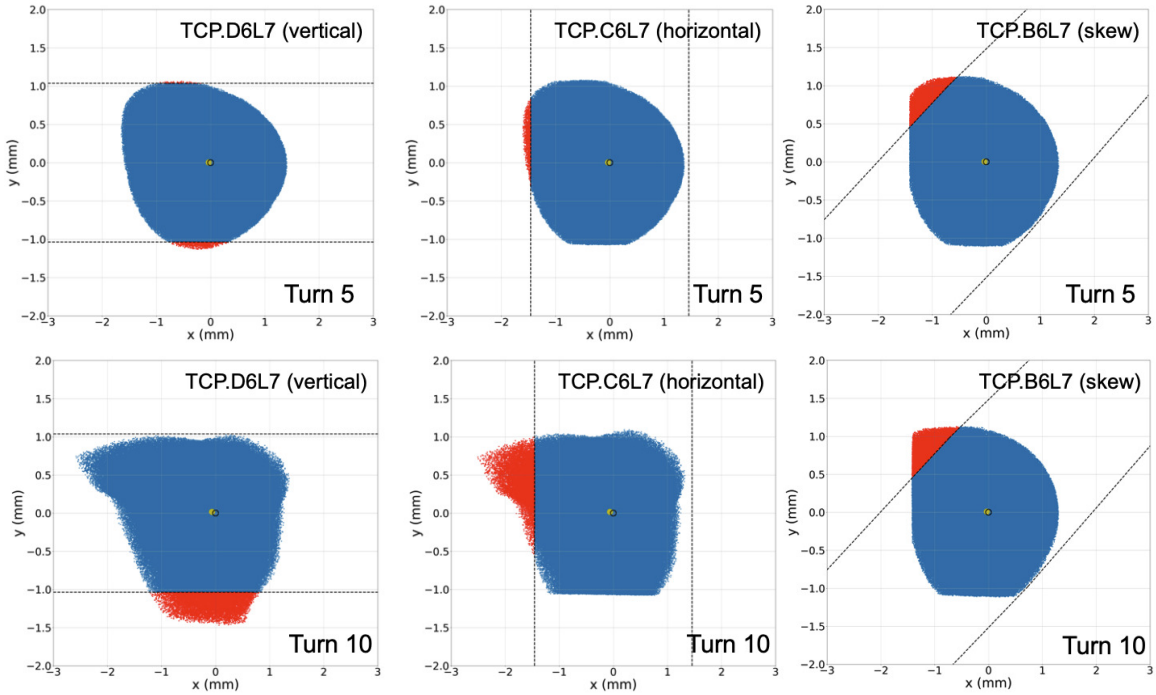

Figure 4: Non weighted beam distributions at the primary collimators shown after 5 and 10 machine turns. The surviving particles are shown in blue, and the particles intercepted at a given collimator are shown in red. The cuts imposed by the collimator jaws are shown as black line. The centroids are shown as a yellow dot.

been probed for each turn at the location of the primary collimators with horizontal, vertical and skew orientation (135°), as shown in Fig. 4. The non-weighted tracked distribution is shown, with the surviving particles at a given turn number shown in blue, and the particles lost at that turn on a given collimator shown in red. One can observe the very strong deformation which develops quickly and confirms the resonant behavior induced by the skew octupolar field component. The beam centroid is shown as a yellow dot, confirming that the orbit excursion is not responsible for the losses. Interestingly, the skew collimator (TCP.B6L7) is dominant in intercepting the beam losses, a unique case among the different fast failures. The beam losses and β-beating results also confirm that the collimation hierarchy is not broken prior to turn 10. The losses for beams with depleted halos are also shown in Fig. 3 and are delayed in time, as expected, for increasing depletion factors. For large depletion factors ($\eta \geq 0.8$), the margin between the BLM threshold and the critical loss level is reduced to a single machine turn. This means that a dedicated interlocking mechanism is absolutely required, as the available margin to trigger the beam dump after a BLM interlock is not sufficient. The results for the relaxed collimation settings (TCP cut at 8.5 σ) lead to the same conclusions, with loss levels delayed in time by one machine turn. A fast dedicated system to detect the erratic must be able to trigger a beam dump before the losses reach critical loss level, which is reached within 450 µs for the most critical case with a non-depleted halo. The interlock signal is sent to the Beam Interlock Controller (BIC) and must then be propagated to the LBDS in IR6. In turn, the LBDS must be synchronized with the abort gap, and the extraction is performed within one turn. Table 2 shows that a dedicated detection system of the erratic must be able to detect the CLIQ discharge and trigger within 167 µs.

Table 2: Duration and timings used to determine the allowed reaction time of the fast interlock.

Onset to damage margin	445 µs
BIS propagation	100 µs
LBDS synchronization	89 µs
LBDS extraction	89 µs
Allowed reaction time	167 µs

CONCLUSION

A spurious CLIQ discharge in the Q2b inner triplet quadrupole in IR5 is found to be the fastest and most critical failure scenario for HL-LHC. For a non-depleted transverse halo, the losses reach the critical loss level (1 MJ) within 450 µs. The margin between failure detection with the BLMs and the critical loss level reaches a single turn (89 µs for 80% halo depletion and more. The origin of these beam losses is found to be the resonant effect of the skew octupolar field component, amplified by the large β-functions and crossing bump at that location. To protect from such failure, a dedicated fast detection mechanism is under developement to detect the erratic CLIQ discharge and trigger a beam dump before the losses reach a critical level.

ISBN: 978-3-95450-227-1 ISSN: 2673-5490 doi:10.18429/JACoW-IPAC2022-WEPOPT013

REFERENCES

[1] O. Aberle *et al.*, "High-luminosity large hadron collider (HL-LHC): Technical design report," CERN, Geneva, Switzerland, CERN Yellow Reports CERN-2020-010, 2020. do:10.23731/CYRM-2020-0010

[2] S. Redaelli *et al.*, "Hollow electron lenses for beam collimation at the high-luminosity large hadron collider (HL-LHC)," *J. Inst.*, vol. 16, no. 3, p. 03042, 2021. do:10.1088/1748-0221/16/03/P03042.

[3] R. Cai, D. Mirarchi, C. Tambasco, and T. Pieloni, "Simulations of particle loss due to hollow e-lens and non-linearities for the HL-LHC," 2020. https://cds.cern.ch/record/2732000

[4] C. Hernalsteens, D. Wollmann, C. Wiesner, and C. Lannoy, "The Effect of a Partially Depleted Halo on the Criticality and Detectability of Fast Failures in the HL-LHC", presented at the IPAC22, Bangkok, Thailand, Jun. 2022, paper WEPOPT014, this conference.

[5] E. Ravaioli, "CLIQ. A new quench protection technology for superconducting magnets," Ph.D. dissertation, University of Twente, Jun. 19, 2015.

[6] B. Lindstrom *et al.*, "Fast failures in the LHC and the future high luminosity LHC," *Phys. Rev. Accel. Beams*, vol. 23, no. 8, p. 08001, 2020.

[7] B. H. F. Lindstrom, "Criticality of fast failures in the High Luminosity Large Hadron Collider," 2021. https://cds.cern.ch/record/2762088

[8] C. Hernalsteens *et al.*, "FailSim: A numerical toolbox for the study of fast failures and their impact on machine protection at the CERN large hadron collider," in *Proc. 12th In. Particle Accelerator Conf. (IPAC'21), Campinas, SP, Brazil*, May 2021, pp. 111–114. do:10.18429/JACoW-IPAC2021-MOPAB022.

[9] G. Valentino *et al.*, "Beam diffusion measurements using collimator scans in the LHC," *Phys. Rev. ST Accel. Beams*, vol. 16, no. 2, p. 021 003, 2013. do:10.1103/PhysRevSTAB.16.021003.

[10] B.Salvachua *et al.*, "Lhc blm threshold model for collimators in IR7 after LS2," CERN, Tech. Rep., 2022. https://edms.cern.ch/document/2719472/2